# Water Availability in Subcutaneous Zone as a Boundary Layer Controlling the Climate-Soil-Vegatation and Groundwater Dynamics: Preliminary Results from Modeling Water Resources in the Seyhan River Basin, Turkey

**Levent Tezcan,[1] Mehmet Ekmekçi [2], Özlem Atilla,**
**M. Evren Soylu, Dilek Gürkan, Orçun Yalçınkaya, Otgonbayar Namkhai**
*International Research Center For Karst Water Resources, Hacettepe University Beytepe 06532 Ankara*
**Sevgi Donma, Dilek Yılmazer, Adil Akyatan, Nurettin Pelen**
*State Hydraulic Works (DSI), District VI, Adana*
**Fatih Topaloğlu,** *Çukurova University, Adana*
**Ahmet İrvem,** *M. Kemal University, Antakya*
*e-mail:*[1,2] tezcan@hacettepe.edu.tr ekmekci@hacettepe.edu.tr

## 1. Introduction

The subcutaneous zone, defined to cover the soil zone and the shallow vadose zone beneath the soil zone. This zone is characterized by intensive biologic activity controlled by the availability of air, water and nutrient. From the standpoint of hydrology, this zone acts as an interface between the surface and subsurface environments. Assuming that infiltration, deep percolation and evapotranspiration are controlled to a great extent by availability of soil water and the vegetation. Similarly, it is assumed that surface runoff can only occur only when saturation is attained in the subcutaneous zone. Based on these facts, it can be state that the availability of water in the subcutaneous zone plays a key role in the climate-soil-vegetation dynamics.

This paper outlines the logic behind the use of the water availability in the subcutaneous zone and the preliminary results obtained from application of a model integrating the climate-soil-vegetation systems to assess the dependency of water resources on these systems in the Seyhan River Basin.

## 2. Subcutaneous Zone as a Boundary Layer

Interactions between hydrological and biogeochemical systems, involves climatic conditions represented by meteorological parameters like precipitation and evaopotranspiration, infiltration as the excess precipitaion from interception and evaporation from surface storage, deep percolation to groundwater system and the factors controlling the biomass including nutrient uptake, decomposition and leaching and weathering.. As depicted I Figure 1, the soil moisture seems to have not only the more linkages than other components, but also linkages with both surface and subsurface environment, implying that the soil zone plays a key role in the climate-soil-vegetation dynamics.

This dynamics can be interrelated within a differential equation that describes the volumetric water change in the soil zone (Rodriguez-Iturbe, 2000).

$$nZ\frac{d\theta}{dt} = I(\theta,t) - E(\theta,t) - D(\theta,t)$$

(1)

Where,

n= porosity, Z: depth of soil zone, θ: soil moisture content, I(θ, t): infiltration into soil, , E(θ, t): evapotranspiration, and D(θ, t): deep percolation to groundwater system.

The terms on the right hand side of Equation 1, are all functions of θ, the soil moisture content. Infiltration depends on the saturation degree of the soil. In other words, infiltration does not exceed the available void volume in the soil during a particular storm. Surface runoff is assumed to tae place only when the substrate is saturated with water, relating the surface runoff with the availability of water in the subcutaneous zone.

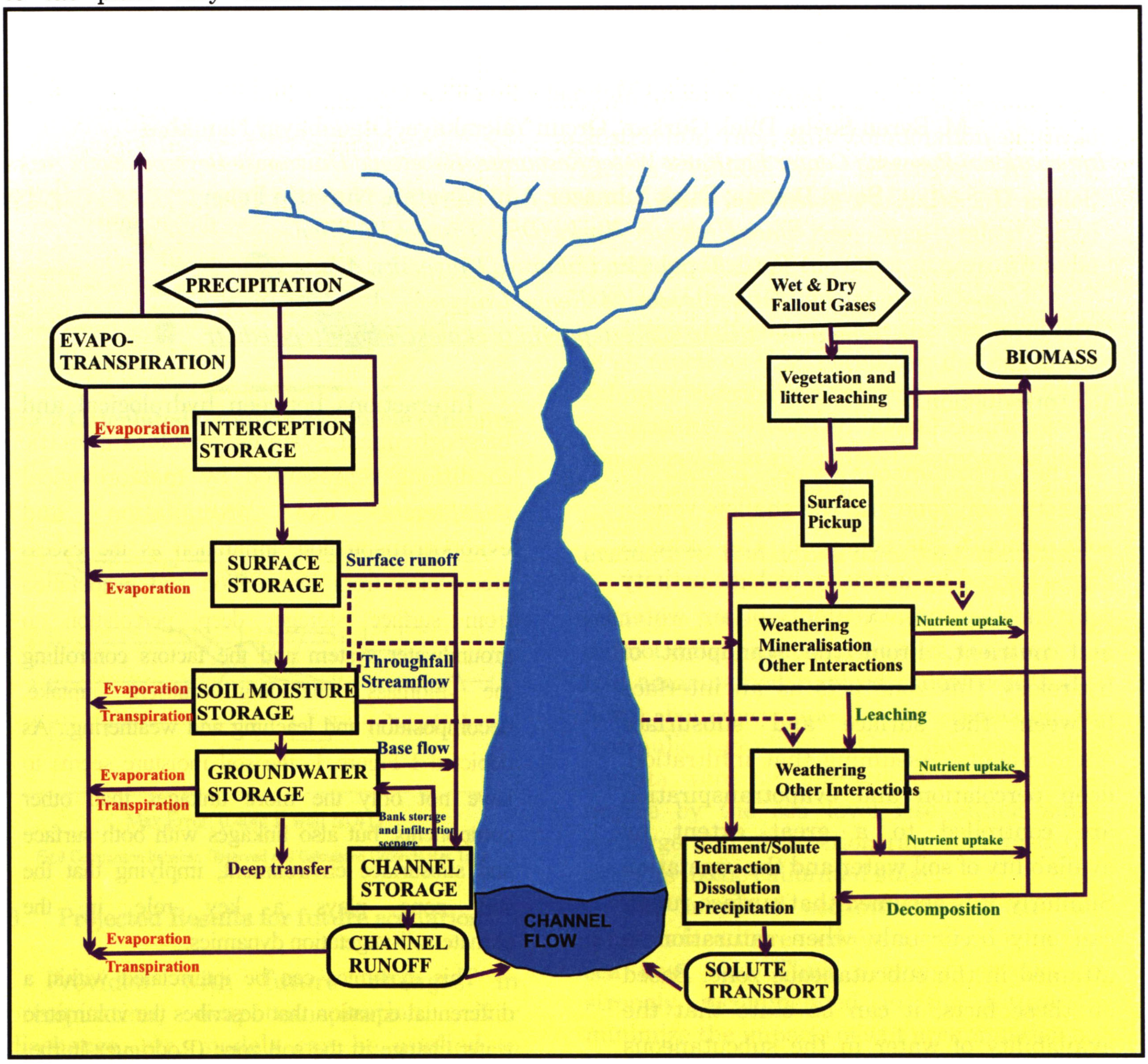


Figure 1. Simplified representation of the interaction of hydrological and biochemical processes operating in a drainage basin [from *Webb and Walling*, 1996: Rodriguez-Iturbe, 2000].

Vegetation and soil characteristics control the evaptranspiration to a large extent. Wilting point and field capacity are known to control the evapotranspiration. However, the rate of evapotranspiration is dependent on the type of vegetation because of different wilting point and the soil moisture allow maximum evapotranspiration vary among different types of vegetation. Evapotranspiration in forested area is quite different from an area covered by herbaceous vegetation even when climatic conditions and soil environments are similar. The last term, deep percolation is apparently nder the control of the saturated hydraulic conductivity, soil water and soil characteristics. This relaton is generally given as Ks $\theta^c$ , where Ks is the saturated hydraulic conductivity, $\theta$ is the soil moisture and the exponent c is a constant dependent on the type of soil. Although the nature of equation 1 may be regarded as stochastic differential equation (e.g. Rodiguez-Iturbe, 2000) because of the fact the precipitation which controls the water content in the subcutaneous zone is a random process, it can be solved by for a certain basin by combining separate solutions for each term. MIKE-SHE (Systeme Hydrologique Europeen), a software combining climate-soilvegetation and groundwater systems was used to assess the interrelations between these systems in the Seyhan River Basin. The code has six modules for snowmelt, evapotranspiration, surface runoff, flow in the subcutaneous zone, channel flow and groundwater flow. The first two are calculated by analytical methods, while the surface runoff and channel flow are simulated by finite difference solution of the 2-D and 1-D Saint-Venant equation, respectively. The unsaturated flow is simulated by the finite difference solution of the 1-D Richards equation. Groundwater flow is simulated by the finite difference solution of the 3-D Boussinesq equation (Abbott et al, 2000). The MIKE-SHE software was used to simulate the surface hydrology of the mountainous Upper Seyhan Basin. The Plain section, called the Lower Seyhan Basin, is rather flat and has no significant surface flow. Therefore, another code that embodies the MODFLOW and MT3DMS in SEAWAT-2000 which also cabaple of simulating the variable density flow and solute transport, enabling simulation of sea water intrusion.

## 3. Preliminary Results from Modeling Studies

The water resources of Seyhan River Basin were investigated within the framework of the ICCAP Project, dividing the basin into two parts: the alluvial plain and the upstream mountainous section. This division was based upon the fact that the plain comprise the major groundwater resources while the upstream section requires methods of surface hydrology though significant karstic aquifers exist in this part of the basin Figure 1.

### 3.1. Impacts of Climate Change of Basin Hydrology

Upstream of the Seyhan Dam was considered as the study area where the impact of climate change on surface hydrology was investigated. This part of the basin covers about 21750 km2. Three main tributaries make the Seyhan River; namely, Cakit, Zamanti and Goksu.

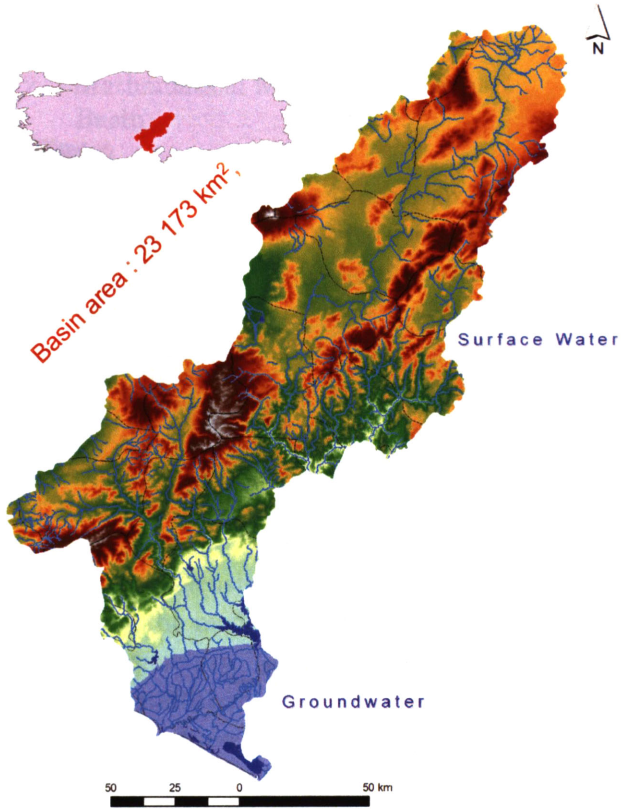


Figure 1. Division of Seyhan River Basin according to type of water resources

The physiography and oro-hydrography of the basin varies from south to north; the lowlands characterizing the south while the north is represented by harsh topography. The Zamanti subbasin, being the largest, requires a special attention due to its relatively complex hydrological structure. The average elevation of this subbasin is about 1250 m. asl., and karstic discharges supply the main contribution to the river flow. The pervious lithological units are generally made of carbonate rocks most of which are extensively karstified. The distribution of the hydrogeological units is depicted in Fig. 2. The response of the basin hydrology to any change in the climatic and inherent vegetative and land-use conditions was studied by modeling approach, which required, first, the hydrological characterization of the basin under the prevailing conditions.

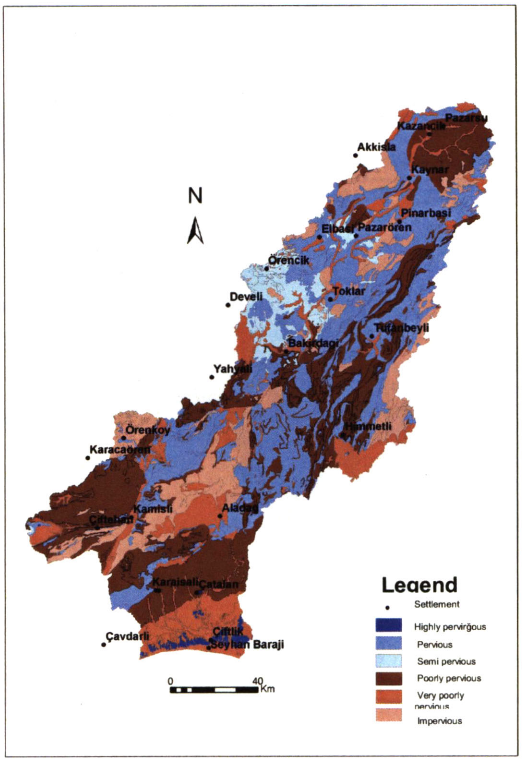


Figure 2. Hydrogeological units in the basin

Description of the basin behavior using tools like mathematical models, then will enable prediction the response of the basin to a future change in any component of the basin. MIKE-SHE/11 (Systeme Hydrologique Europeen) a deterministic and distributed parameter model, integrating surface and subsurface flow and transport processes was utilized toward this purpose (Abbot et al., 1986).

### 3.1.1 Preparation and Processing Relevant Data

The available data were designated, digitized and transferred to a geographical information system software as required by the MIKE-SHE model. Hydro-meteorological data such as flow rates, rainfall (Fig. 3) and snow cover were input to the database, topographical, geological maps, soil map (Fig. 4) were digitized and given as separate layers. The basin boundaries were defined according to the topographical divide. The model parameters such as precipitation, evapo-transpiration and surface run-off were defined and transferred to the model.

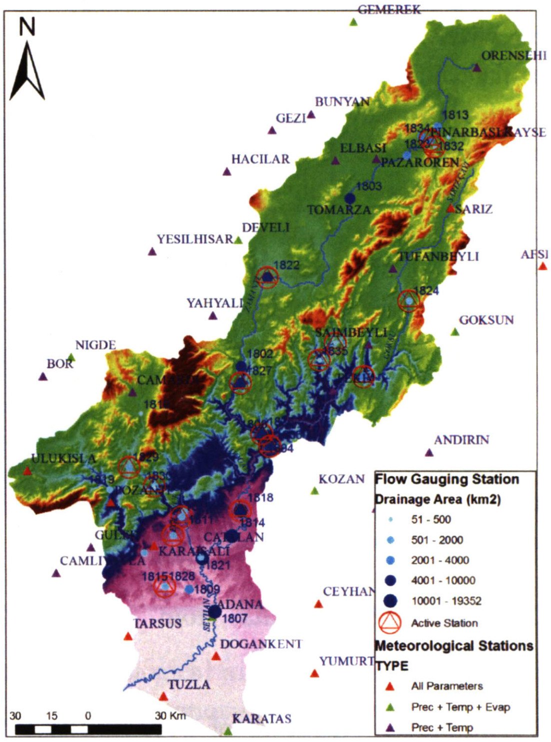


Figure 3. Hydrometeorological station whose data were used in the model.

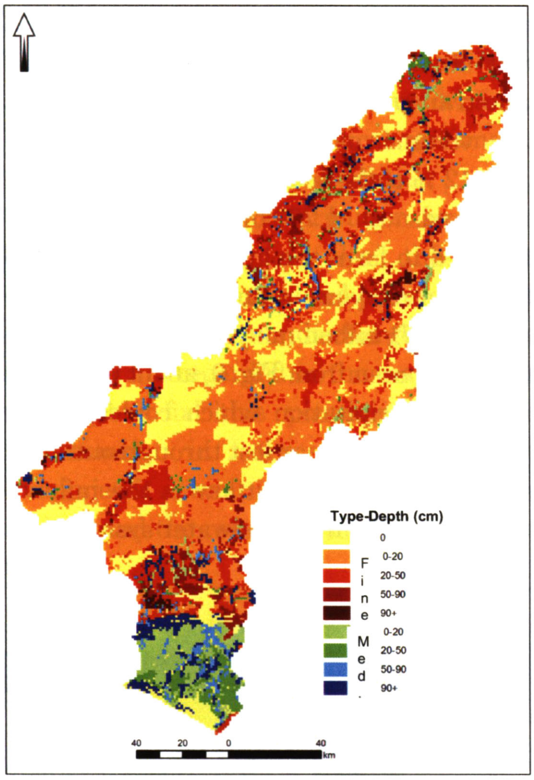


Figure 4. Soil map (yellow: fine and thin, blue: coarse and thick)

Vegetation and leaf area index (LAI) were also defined and transferred to the model (Fig. 5). Calibration of the model was based on the observed flow rates at certain sections of the river system. Prediction of the response of the basin to decrease in precipitation and increase in temperature and evapo-transpiration was then made by running the model for changes forecasted by the GCM.

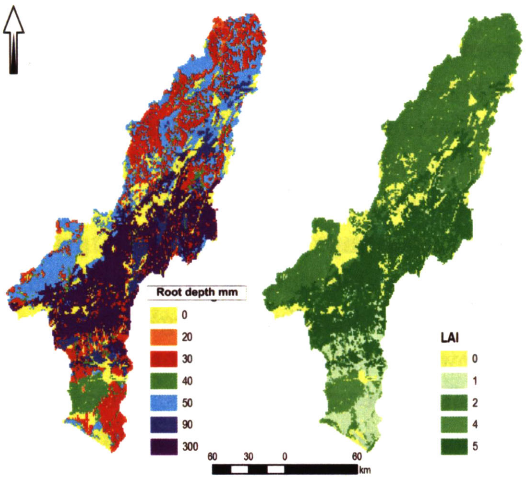


Figure 5. Root depth and LAI in the basin

### 3.1.2. Mathematical Model of the Seyhan Basin

The basin was discretized into 216x299 finite difference grids of 1 km2 each. The boundary of the basin was defined in the model by assigning the a value indicating impervious unit in cells that fall on the divide. MIKE-SHE computes the areal precipitation either by interpolation or by Thiessen polygons. Daily precipitation data of 13 stations were input to the model as time series (Fig. 6).

The evapo-tarnsipration is similarly computed by the model in two ways: 1) the water budget in vadose zone 2) Penman-Monteith method for potential and Leaf Area Index approach for actual evapo-transpiration. Due to the lack of available data to allow the water budget approach, the Penman-Monteith method was used and the leaf area index was utilized with the combination of the root depth (see Fig. 5). The time series of daily potential evapotranspiration is given in Fig 7.

River. As seen in Fig. 8. the correlation between the observed and calculated flow rates is poor. The extent of the model area, lack of adequate meteorlogical stations to represent the precipitation and evapo-transpiration distribution over the basin accounting for also the great differences in elevation and the significant contribution of karstic discharges into the river flow are regarded as the major factors responsible for this poorness. However, adjustment in the water budget components was realized to better understand the role karstic effluents in the basin.

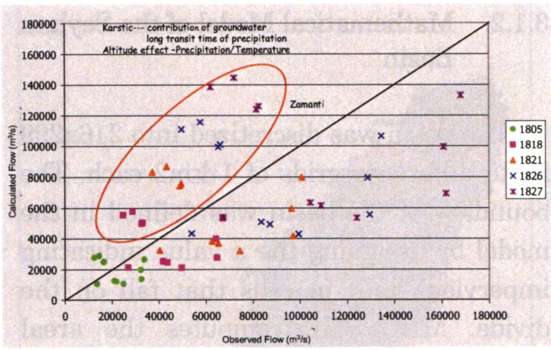


Figure 8. Correlation between observed and calculated flow rates

### 3.1.4. Water Budget

The water budget components calculated by the model for the period between 1980 and 2000 are tabulated in Figure 9. According to this calculation, about 40 % of the precipitation is lost by evapo-transpiration. This rate corresponds to a volume of 15.89 billion m3/year. About 12 % of the total precipitation which corresponds to 4.76 billion m3/year is infiltrated to form the groundwater. About 5.94 billion m3/year is stored in the vadose zone and 3.71 billion m3/year is the surface runoff. As seen from Fig. 9, about 0.6 % of the total precipitation which corresponds to 0.24 billion m3/year lost through outflow from the basin. This outflow is the inflow to the Adana Plain groundwater system.

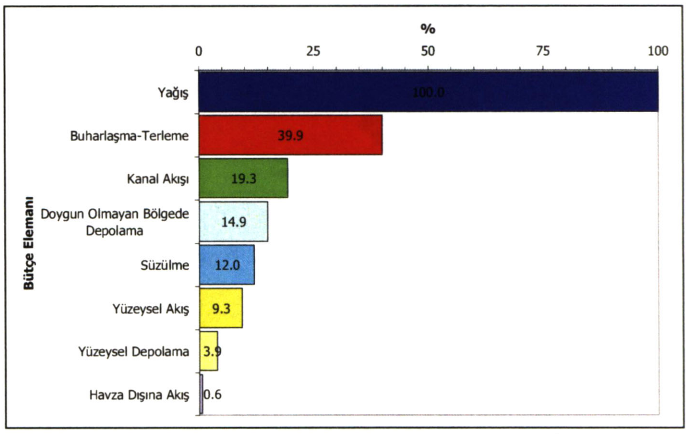


Figure 9. Percentages of water budget components for the period 1980-2000

## 4. Impacts of Climate Change on Adana Plain Aquifer

The Adana alluvial plain, constitutes the major groundwater resources in the Seyhan River Basin (Figure 10). Following the hydrogeological characterization of the Adana alluvial plain, the conceptual model was transferred to the mathematical models. Sea water intrusion was also considered in the conceptual model. Therefore, in addition to the groundwater flow model, the seawater intrusion was also transferred to a mathematical model and run together with the groundwater flow model. MODFLOW (MMcDonald & Harbaugh, 1998) was used to simulate the groundwater flow while the sea water intrusion was simulated by SEAWAT-2000 (Langevin, et al., 2003), integrated with MODFLOW.

River. As seen in Fig. 8. the correlation between the observed and calculated flow rates is poor. The extent of the model area, lack of adequate meteorlogical stations to represent the precipitation and evapo-transpiration distribution over the basin accounting for also the great differences in elevation and the significant contribution of karstic discharges into the river flow are regarded as the major factors responsible for this poorness. However, adjustment in the water budget components was realized to better understand the role karstic effluents in the basin.

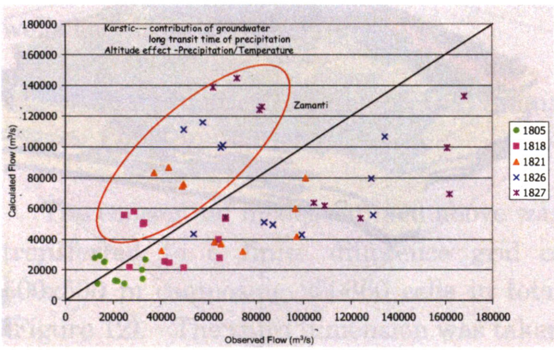


Figure 8. Correlation between observed and calculated flow rates

### 3.1.4. Water Budget

The water budget components calculated by the model for the period between 1980 and 2000 are tabulated in Figure 9. According to this calculation, about 40 % of the precipitation is lost by evapo-transpiration. This rate corresponds to a volume of 15.89 billion m3/year. About 12 % of the total precipitation which corresponds to 4.76 billion m3/year is infiltrated to form the groundwater. About 5.94 billion m3/year is stored in the vadose zone and 3.71 billion m3/year is the surface runoff. As seen from Fig. 9, about 0.6 % of the total precipitation which corresponds to 0.24 billion m3/year lost through outflow from the basin. This outflow is the inflow to the Adana Plain groundwater system.

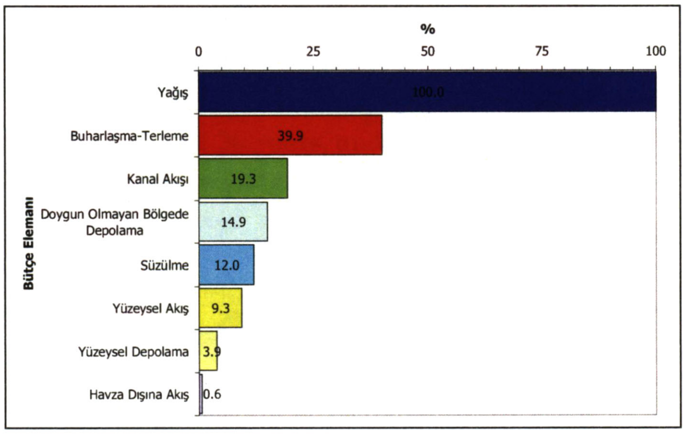


Figure 9. Percentages of water budget components for the period 1980-2000

## 4. Impacts of Climate Change on Adana Plain Aquifer

The Adana alluvial plain, constitutes the major groundwater resources in the Seyhan River Basin (Figure 10). Following the hydrogeological characterization of the Adana alluvial plain, the conceptual model was transferred to the mathematical models. Sea water intrusion was also considered in the conceptual model. Therefore, in addition to the groundwater flow model, the seawater intrusion was also transferred to a mathematical model and run together with the groundwater flow model. MODFLOW (MMcDonald & Harbaugh, 1998) was used to simulate the groundwater flow while the sea water intrusion was simulated by SEAWAT-2000 (Langevin, et al., 2003), integrated with MODFLOW.


Figure 10. Location map of the study area

Following calibration runs, the models were run to simulate the groundwater flow and solute transport (sea water intrusion) for two climate change scenarios. The vulnerability of the plain aquifer system was then evaluated and interpreted in terms of ground water potential and quality.

### 4.1 Hydrogeological Conceptual Model

The Berdan-Tarsus river and Ceyhan River borders the study area from the west and east respectively. The plain aquifer covers an area of about 2271 km$^2$, extending between these borders. Water demand for irrigation in the plain is supplied to a great extent from the Seyhan Dam Lake that borders the study area from the north. Therefore, only a certain number of boreholes were drilled, most of which are located in the northern part of the plain to supply water to the Adana Metropolitan city. However, after drip-irrigation system became attractive to the farmers in the plain, a few boreholes are drilled in the southern part of the plain. The data of these boreholes were used in conceptualizing the groundwater system.

The geohydrologic characterization of the plain aquifer system was based upon the 203 well logs. Depth of boreholes drilled at the northern part does not exceed 100 m., whereas the boreholes at the south are deeper; 363 m. the deepest. The lithological configuration of the plain aquifer system is depicted in Figure 11.

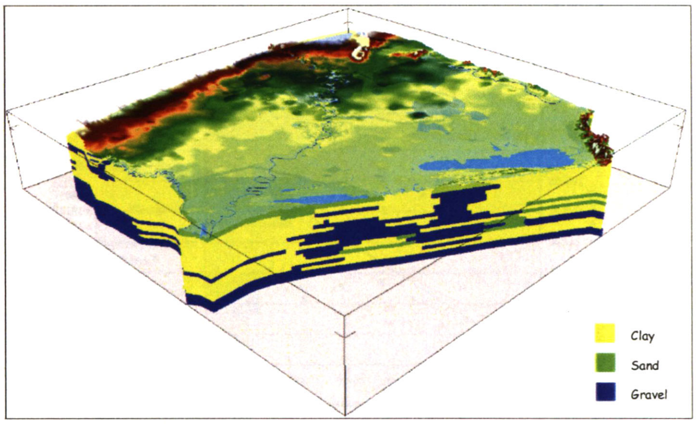


Figure 11. 3-D distribution of lithologic units in plain

The Tarsus-Berdan river that borders the area from the west, flows over a thick clay (impervious) layer. Similarly the Ceyhan River flows over a thin sandy layer underlied by again a thick clayey layer. The northern part of the plain is covered by a succession of gravel-clay-gravel.

Detailed study of the well logs suggests that it is difficult to distinguish more than one aquifers, but instead, it is more realistic to consider one heterogeneous aquifer with vertical and horizontal interfingering layers of pervious and impervious deposits; which is also supported by the type of the depositional environment. The 3-D distribution of the clay, sand and gravel layers were transferred to the mathematical model assigning a distinctive hydraulic coefficient for each. The aquifer is recharged through direct rainfall onto the areas where coarse deposits are exposed, from seepage from the Seyhan River where the bed is composed of pervious material and through inflow the northern boundary. Because the amount of the inflow through the northern boundary is difficult to predict and any prediction would associate significant uncertainty, the boundary condition was defined based upon the groundwater level measurements in the boreholes close to this boundary. This provided that recharge through this boundary is computed by the model based on the gradient changes. Discharge of the aquifer occurs as the outflow into the sea, effluent flow to the Seyhan River where hydrogeologic conditions are appropriate, and as groundwater abstraction through wells and drainage canals.

### 4.2. Mathematical Model of the Adana Plain Aquifer

The conceptual model outlined above was transferred to a finite difference grid of 500x500 m composing 250860 cells in total (Figure 12). The third dimension was taken between elevations of 20 m. above and 320 m below sea level. 20 model layers of 20 m thickness each were defined to represent the vertical dimension. The model was run for steady state conditions first to achieve calibration. The simulation was performed for three periods starting from 1990. The first run was performed to simulate the present conditions for 10 years, thus having the conditions of the year 2000 computed by the model. The result of this run is given in Figure 4. The second run was to simulate the system for the first scenario that considers that an annual sea level rise of 2 mm for the next 20 years, thus attaining a total rise of 40 cm at the end of 2020. The third run simulated another 50 years. The rate of sea level rise was increased for this period. And the total rise at the end of the period was 80 cm. simulation for 2000.

The boundary condition at the south where the aquifer is in contact with the sea was taken as "constant head-concentration boundary" for the first 10 years; whereas this boundary was changed to "variable head-concentration boundary" during the second and third periods where the system is affected by the climate change. The concentration of the sea water was taken as 19200 mg/l of Cl from chemical analysis of the sea water.

The constant-head at the northern part was taken as 20 m. on average. No concentration was given at this boundary. The impact of the climate change was reflected by decreasing the head by 10% to 18 m for the first 20 years, and to 15 m for third period. The recharge rate was defined based upon the excess water calculated from the hydrometeorologic data. Regarding the time-scale of the study, recharge was input on annual basis to the model. The impact of the climate change was reflected by decreasing the rate of recharge by 20 % for the period 2000-2020 and by 40% for the period 2020-2070. Uniform recharge over the plain was assumed for this preliminary run. The water depth at Seyhan River was taken 10 cm on the average. Discharge as outflow to the sea is computed by the model taking the constant-head approach. The model also calculates discharges through drainage canals, considering the hydraulic conductivities, bottom elevation and hydraulic gradient. Abstraction was estimated based on the assumption that demand for groundwater will increase by 20% during the third period.

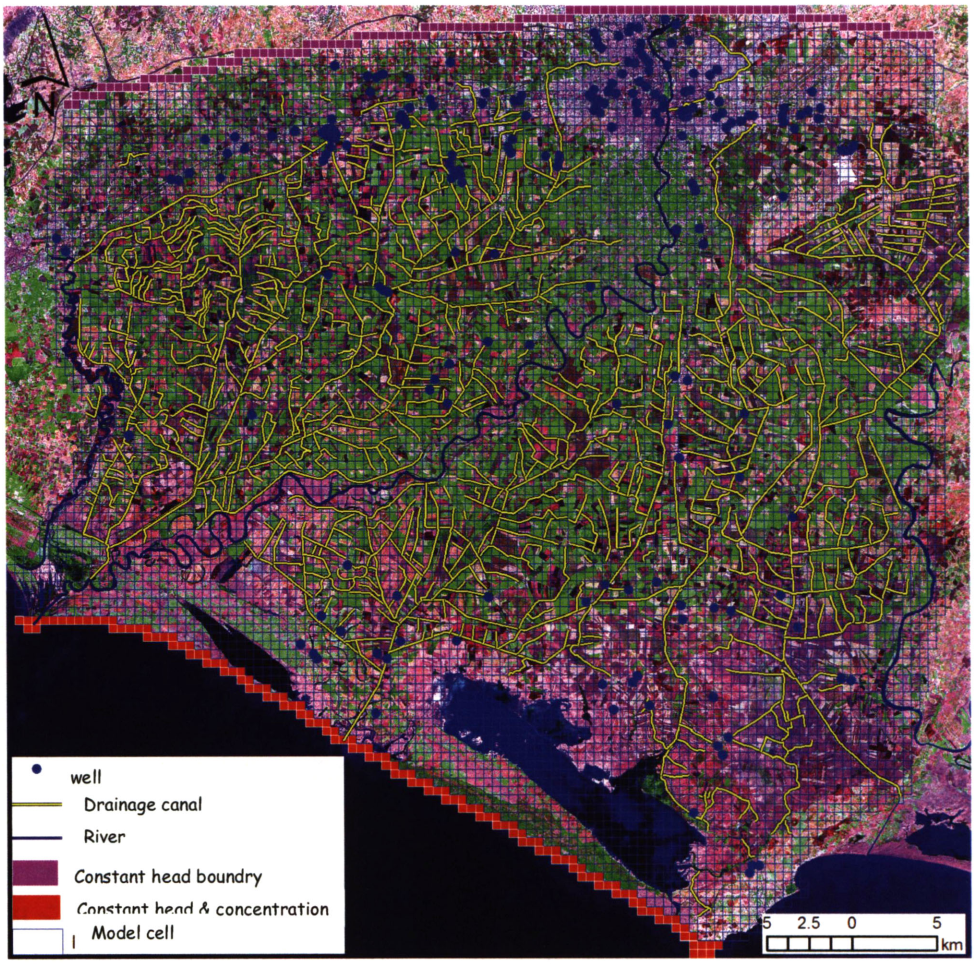


Figure 12. Grid mesh and boundary conditions in the modeled area

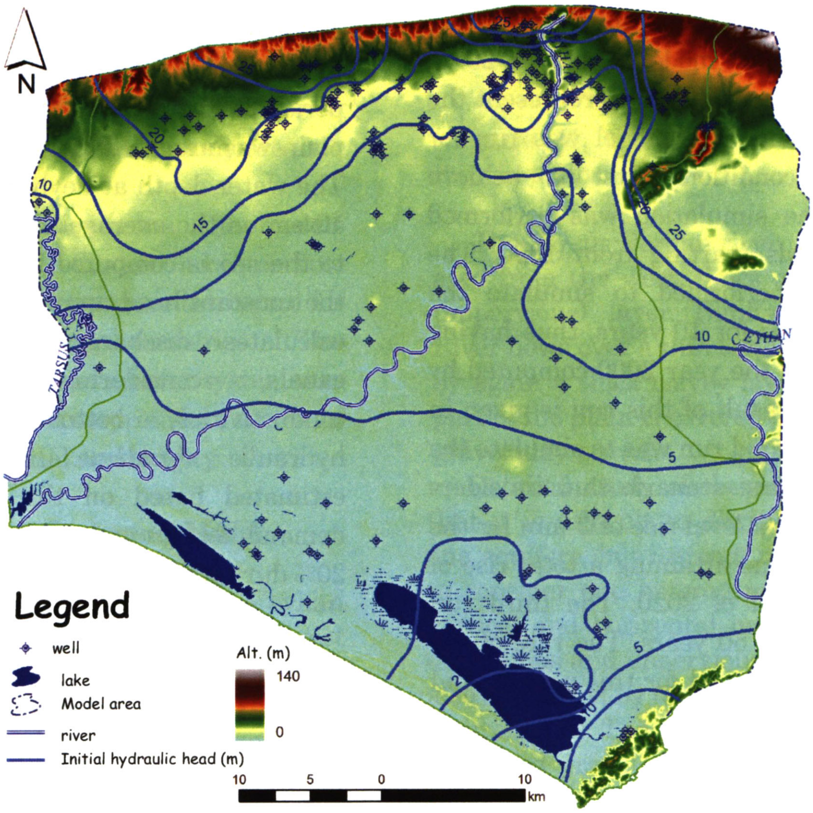


Figure 13. Head distribution from steady-state

### 4.3. Results

Simulations described above produced results in the form of head and concentration distributions for 80 years. Head and concentration distributions for some years are depicted in Fig. 14 and Fig. 15, respectively. The results revealed that and water consumption affects the head distribution significantly. Similarly, sea water intrusion will pose a problem, although it is not severe. Finally the water budget components calculated by the model and the decline in storage are given in Fig. 16 and Fig.17, respectively.

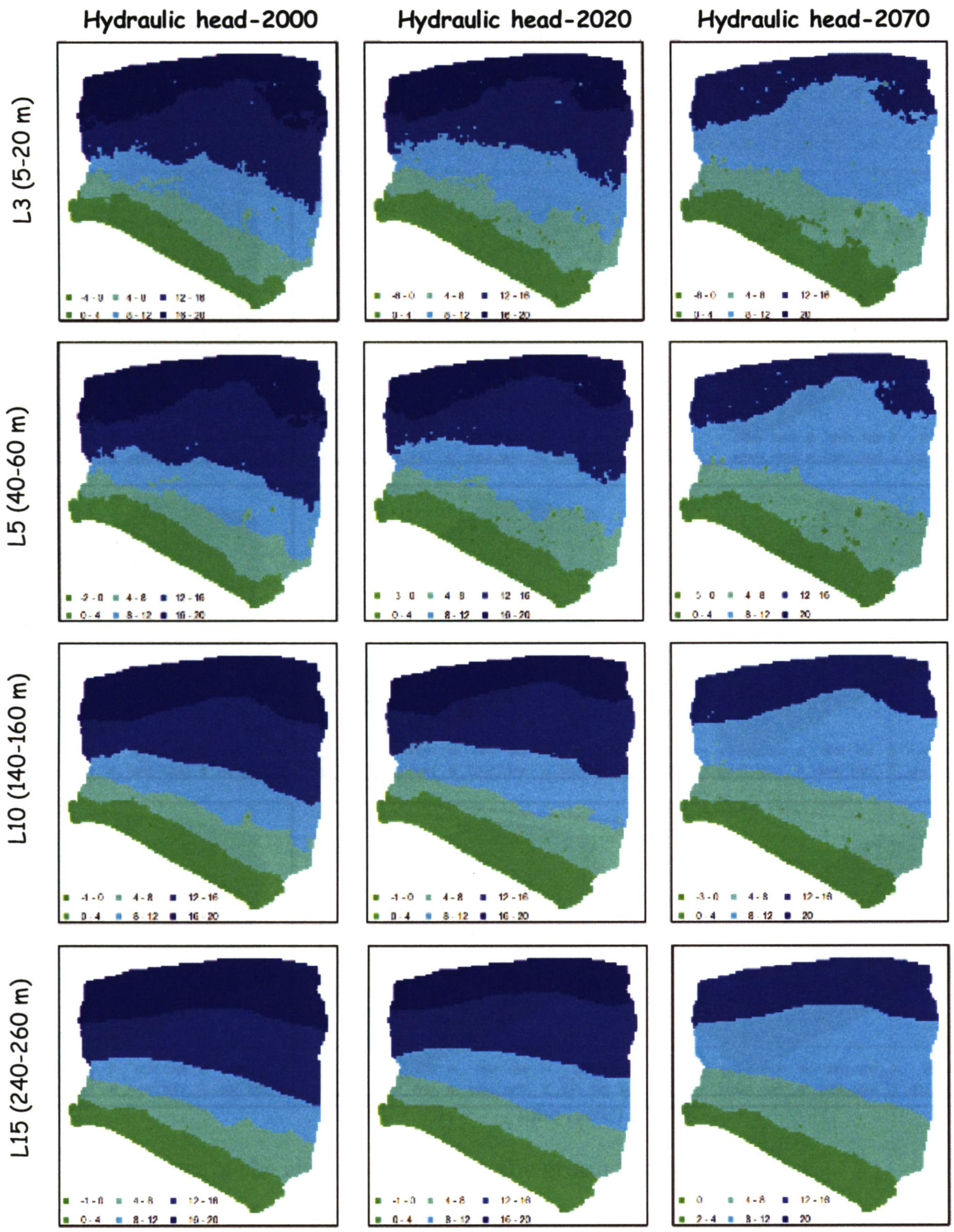


changes in hydro-meteorologic conditions

Figure 14. Head distribution at different layers after simulation the climate change (2000, 2020 &2070)

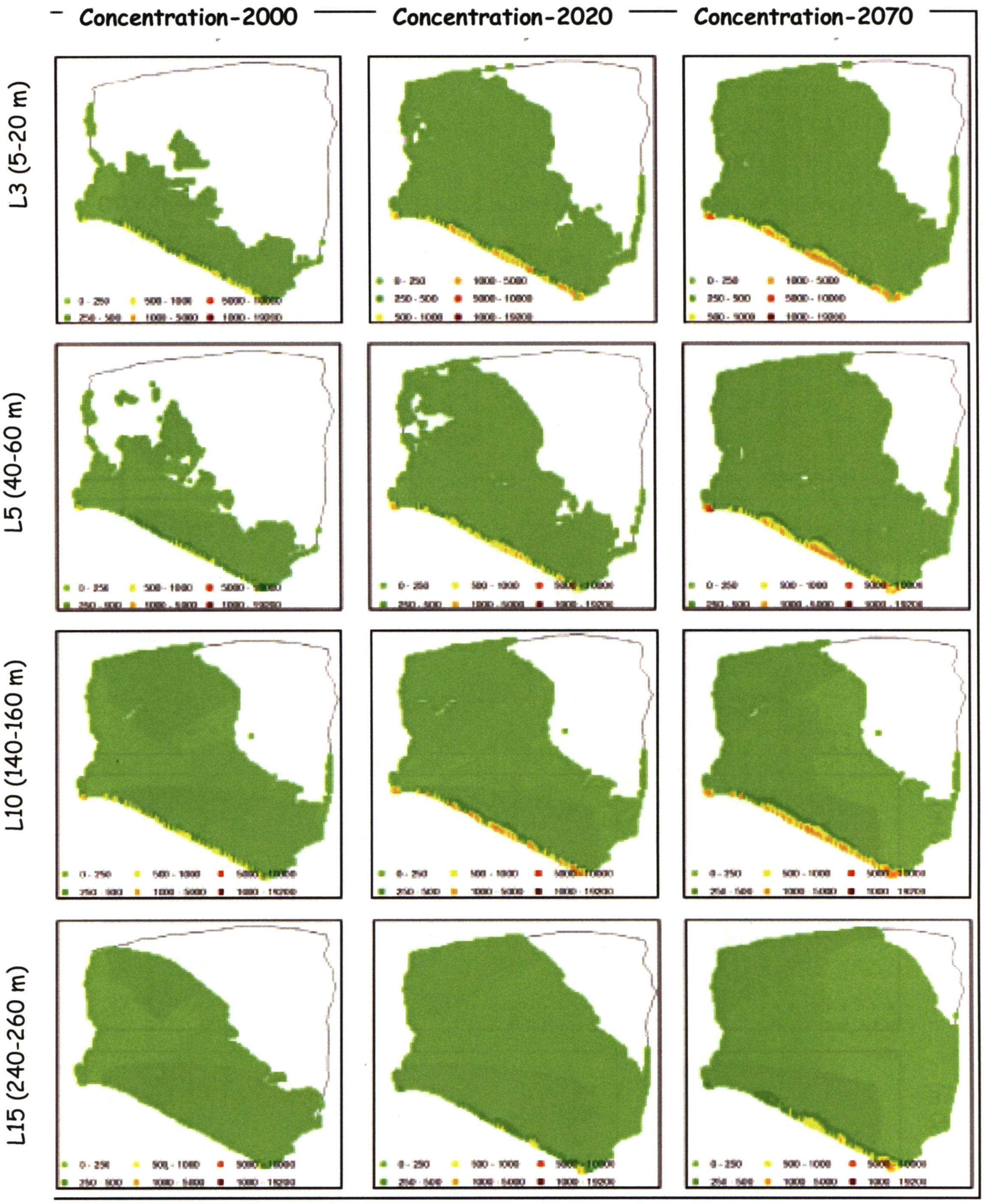


Figure 15. Chloride concentration distribution at different layers after simulation the climate change (2000, 2020 &2070)

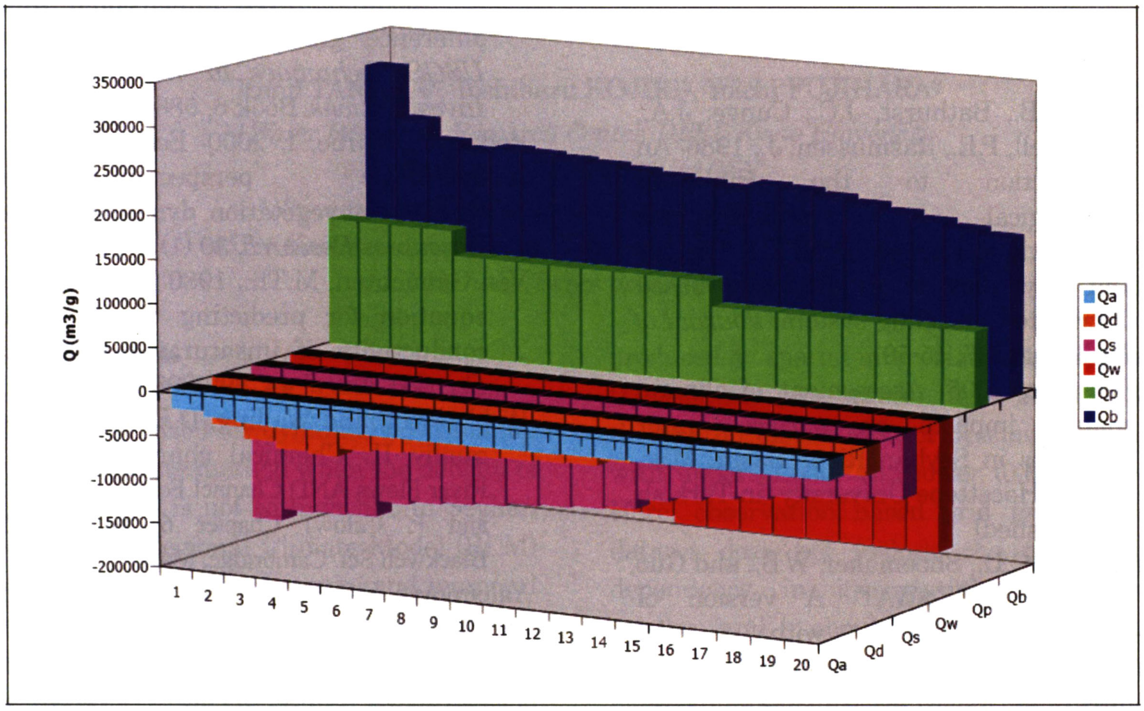


Figure 16. Components of the water budget calculated by the model (Qb: inflow from the northern border, Qp: recharge from precipitation, Qw: abstraction by wells, Qs: outflow to the sea, Qd: drainage by drainage canal, Qa: effluent flow to Seyhan river)

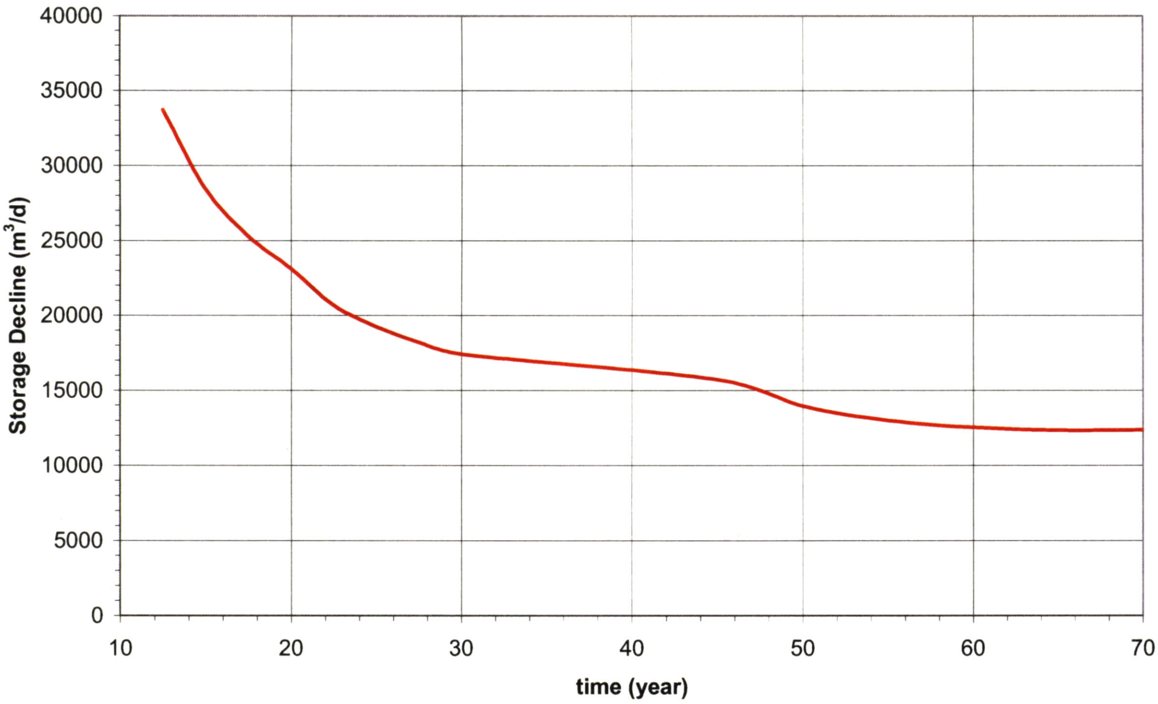


Figure 17. The impact of the climate change on the ground water storage

## 5. References


Abbott, M.B., Bathurst, J.C., Cunge, J.A., O'Connell, P.E., Rasmussen, J., 1986: An introduction to the European hydrological system-Systeme hydrologique Europeen, SHE 1. History and phylosopy of a physically based distributed modeling system. *Journal of Hydrology*, **87**, 45-59.

Gürkan, D., 2005: Assessment of climate change impacts on surface water resources in Seyhan River Basin, MSc. Thesis, Hacettepe University (in Turkish, unpublished)

Langavein, C.D., Shoemaker, W.B., and Guo, W., 2003: SEAWAT: A version of MODFLOW-2000 with the variable-density flow process and the integrated MT3DMS transport process. *USGS Water Resources Publication.*

McDonald M.G. and Harbough, A.W., 1988: A modular three dimensional finite difference ground water flow model, *USGS Techniques in Water Resource Investigations*, Book 6, 586.

Rodriguez-Iturbe, I, 2000: Ecohydrology: A hydrologic perspective of climate-soil-vegetation dynamics. *Water Resources Research*, 30 (1), 3-9.

Van Genuchten, M.Th., 1980: A closed-form equation for predicting the hydraulic conductivity of unsaturated soils. *Soil Sci. Soc. Am. J.* **44**, 892-898

Webb, W.B., and Walling, D.E. 1996: Water qualiy II. Chemical characteristics. In River Flows AND Channel Forms (ed. G Petts and P. Calow) Chapter 6, pp 102-129, Blackwell Sci. Cambridge, Mass.

Yalcınkaya S.O., 2005: The impacts of the climate change in Adana plain on the groundwater level and sea water intrusion, MSc. Thesis, Hacettepe University (in Turkish, unpublished)